Analysis of the Omega Diagram for Cosmic Microwave Background Anisotropy and Type Ia Supernovae

Vivek Venkatachalam

under the direction of
Dr. Edmund Bertschinger
Massachusetts Institute of Technology

Research Science Institute
July 31, 2001

Abstract

The fate of the universe depends largely on its energy density relative to the critical energy density. This energy density consists of both matter energy and vacuum energy (also known as dark energy). Experimental data from Type Ia supernovae and from cosmic microwave background anisotropy measurements, when plotted on the Omega diagram as a graph of Ω_Λ versus Ω_m, conveniently constrains the values of the two Ω parameters to $\Omega_\Lambda \approx 2\Omega_m \approx 2/3$. This paper presents a physical explanation to elucidate the relative positions of these constraints and their uncertainties.

1 Introduction

Two types of energy are thought to fill the universe today. The first is non-relativistic matter energy, which consists of both baryonic matter (the well-known type of matter composed of protons, neutrons and electrons) and non-baryonic dark matter. The second is vacuum energy, the cosmological constant that uniformly pervades all space and is marked by its negative pressure.

The densities of these two forms of energy define two cosmological parameters that determine, in large, the structure and fate of the universe: $\Omega_m = \rho_m/\rho_c$, the ratio of the mean mass density to the critical density required for a flat universe, and $\Omega_\Lambda = \rho_\Lambda/\rho_c$, the ratio of vacuum energy density to the critical density. If $\Omega_m + \Omega_\Lambda = 1$, then the universe has a flat spatial geometry. If $\Omega_m + \Omega_\Lambda > 1$ or $\Omega_m + \Omega_\Lambda < 1$, then the universe has a closed or open spatial geometry, respectively. If $\Omega_\Lambda = 0$, then a closed universe will eventually recollapse while flat and an open one will expand forever. If $\Omega_\Lambda > 0$, then a closed universe may expand forever [1, 2]. Figure 1 diagrams these facts.

Prior to the recent measurements of the cosmic microwave background and Type Ia supernovae, constraints on the omegas had already been established. Gravitational mass measurements in galaxies and galaxy clusters constrain Ω_m to 0.4 ± 0.2 [3], and a variety of constraints, including gravitational lens tests, fix $\Omega_\Lambda \leq 1$ [4].

Recent developments have placed even tighter constraints on the possible values of Ω_m and Ω_Λ. Two groups of astronomers have used the magnitude-redshift relation of Type Ia supernovae (SNe Ia) to conclude that the cosmic expansion is speeding up, requiring $\Omega_m + 2\Omega_\Lambda > 0$ [1]. The contributions of Ω_m and Ω_Λ were also constrained to $\Omega_m \approx 1 - \Omega_\Lambda$ by cosmic microwave background (CMB) anisotropy observations from the cosmic photosphere made by the Maxima [5], Boomerang [6], and DASI [7] experiments. The results of both the CMB anisotropy and SNe Ia projects, when plotted together, produce Figure 1.

In Figure 1, it can be seen that the two plots intersect nearly orthogonally. The inter-

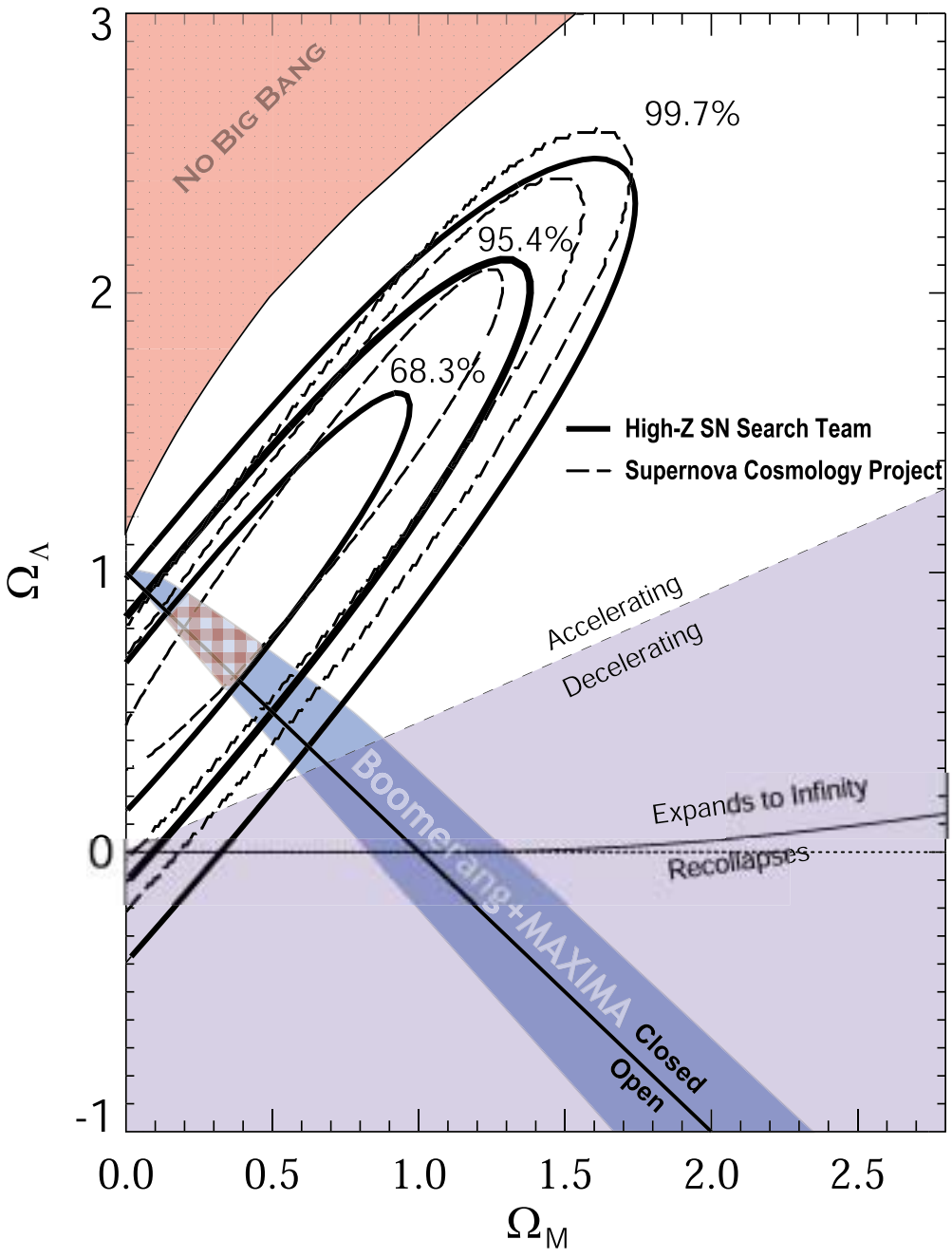

Figure 1: The Omega Diagram: Ω_m vs. Ω_Λ error ellipses for constraints from CMB anisotropy (labeled CBR anisotropy here) and Type Ia supernovae. The line for $\Omega_{tot} = 1$ has been plotted. It should be noted that all three constraints are satisfied when Ω_m and Ω_Λ have values in the checkered region. This figure also shows how different values of Ω_m and Ω_Λ will affect the structure and fate of the universe. (Diagram from [8])

section of the major axes of the error ellipses for the two plots occurs at $\Omega_m \approx 1/3$ and $\Omega_\Lambda \approx 2/3$, indicating that vacuum energy contributes 2/3 of the total energy in the universe. Furthermore, the orthogonality of the uncertainties results in a small region of error for these values of Ω_m and Ω_Λ. These measurements give the strongest evidence thus far that the universe will expand forever, and that the rate of expansion is increasing [1].

This paper will provide a physical and mathematical argument that explains the results of the SNe Ia and CMB projects in Figure 1. This will be done by first developing two tools, the Friedmann Equation and the Robertson-Walker metric, and then subsequently using them to explain the orientation of uncertainties in Figure 1.

2 The Friedmann Equation and its Implications

This section will sketch a derivation of the Friedmann equation following an outline similar to that presented in [10]. Four assumptions will be made. First, it will be assumed that Newton's Laws are valid on scales much smaller than the Hubble length. Second, it will be assumed that mass is conserved and that vacuum energy and radiation are negligible. Third, it will be assumed that the universe is both homogeneous and isotropic. Finally, it will be assumed that the expansion of the universe is uniform, i.e. $r_1(t)/r_2(t) =$ constant where $r_1(t)$ and $r_2(t)$ are distances of two test particles from an arbitrarily chosen center of the expansion. We will treat a small portion of the universe as a sphere with uniform density and fixed mass.

Consider a test particle, at distance $r(t)$ on the outside of the sphere. The particle's equation of motion is given by

$$m\ddot{r}(t) = \frac{-GMm}{r^2(t)}, \tag{1}$$

where G is the gravitational constant, M is the mass enclosed by the sphere, and m is the mass of the test particle. Multiplying both sides of equation (1) by $\dot{r}(t)/m$, taking the time

integral, and using the fact that $M = \frac{4}{3}\pi r^3(t)\rho(t)$ is a constant yields

$$\frac{\dot{r}^2(t)}{2} = \frac{4}{3}\pi G r^2(t)\rho(t) - \frac{\kappa}{2}, \tag{2}$$

where κ is an integration constant and $-\kappa/2$ corresponds to the energy per unit mass of the test particle.

Now let $a(t)$, the cosmic scale factor, be defined as $a(t) \equiv r(t)/r_0$. (Subscript 0's denote present values.) This $a(t)$ provides an overall scaling for the separation between all objects in a uniformly expanding universe. Let the curvature, k, be defined as $k = \kappa/r_0^2$, and let the Hubble parameter $H(t)$ be defined as $H(t) \equiv \dot{a}(t)/a(t)$. By substituting these parameters, we can eliminate explicit dependance on r_0 and generalize the argument from a test particle to the entire universe. Dividing equation (2) by $r^2(t)$ and using the above definitions yield

$$H^2(t) = \left[\frac{\dot{a}(t)}{a(t)}\right]^2 = \frac{8\pi G}{3}\rho(t) - \frac{k}{a^2(t)}. \tag{3}$$

Equation (3), known as the Friedmann equation, is a statement about cosmic expansion, as it describes the relative motion of all bodies on large scales. It shows how the density (ρ) and curvature (k) of the universe affect its size and fate. If $a(t) \to 0$ at any time, then the the universe collapses in a big crunch. If $a(t) \to \infty$ as $t \to \infty$, then the universe will expand without bound. The observable universe is thought to have begun expansion about 14 Gyrs ago at time $t = 0$ when $a = 0$.

Remarkably, although the above derivation uses only non-relativistic physics, equation (3) is still valid in general relativity and for all types of matter and energy [10]. In a relativistic universe, there are three contributions to ρ. Thus, ρ can be separated into $\rho_{tot} = \rho_m + \rho_\Lambda + \rho_r$, where ρ_m is the matter density, and ρ_r and ρ_Λ are the radiation energy density and vacuum energy densities respectively, both multiplied by c^{-2}. This factor of c^{-2} will always be assumed for the remainder of this paper to maintain the correct units of mass/volume for ρ.

Now define

$$\Omega_{m,\Lambda,r}(t) \equiv \frac{8\pi G}{3H^2(t)}\rho_{m,\Lambda,r}(t) \tag{4}$$

$$\Omega_k(t) \equiv -\frac{k}{a^2(t)H^2(t)}. \tag{5}$$

Using the above definitions, the Friedmann equation can be rewritten as

$$1 = \Omega_m(t) + \Omega_\Lambda(t) + \Omega_r(t) + \Omega_k(t). \tag{6}$$

At late times, Ω_r is negligible. We therefore see that for a flat ($k = 0$) universe, $\Omega_m + \Omega_\Lambda = 1$. This reference line is plotted on Figure 1.

To simplify calculations later on, another alternate form of equation (3) will be presented. It is obtained simply by changing variables from the proper time variable t to the conformal time variable τ, where $dt = a(t(\tau))\ d\tau \equiv a(\tau)\ d\tau$:

$$H^2(\tau) = \left(\frac{1}{a^2}\frac{da}{d\tau}\right)^2 = \frac{8\pi G}{3}\rho(\tau) - \frac{k}{a^2(\tau)}. \tag{7}$$

Because matter density is inversely proportional to volume with a scale factor of a^{-3}, vacuum energy density is constant, and radiation density is inversely proportional to a^4, the total energy density is

$$\rho(\tau) = \frac{3H_0^2}{8\pi G}\left[\Omega_m a^{-3}(t) + \Omega_\Lambda + \Omega_r a^{-4}(t)\right], \tag{8}$$

where $\Omega_i = \Omega_i(\tau_0)$ and $a = a(\tau)$. One can now rewrite equation (7) as

$$\left(\frac{da}{d\tau}\right)^2 = H_0^2\left(\Omega_m a + \Omega_\Lambda a^4 + \Omega_r - \frac{ka^2}{H_0^2}\right) \tag{9}$$

By convention, $a_0 \equiv 1$, so one can make the substitution $-k/H_0^2 = \Omega_k(t_0) = \Omega_k =$

$1 - \Omega_m - \Omega_\Lambda - \Omega_r$. Making this substitution and subsequently solving for $H_0\tau(a)$ yields:

$$H_0\tau(a) = \int_0^a \frac{dx}{\sqrt{\Omega_m x + \Omega_\Lambda x^4 + (\Omega_r h^2)h^{-2} - \Omega_k x^2}}, \tag{10}$$

To simplify things later on, we have introduced the dimensionless Hubble constant $h \equiv H_0/(100 \text{ km s}^{-1} \text{ Mpc}^{-1})$. Equation (10) will be central to the discussion of both cosmic microwave background and supernovae in later sections.

3 The Robertson-Walker Metric

The other tool that will be necessary to analyze the results of the SNe Ia and CMB measurements is the Robertson-Walker spacetime metric.

We begin with the metric for flat spacetime, which, in rectangular coordinates, is given by

$$ds^2 \equiv -(c\ dt)^2 + dx^2 + dy^2 + dz^2. \tag{11}$$

This metric assumes that the effect of gravity is negligible.

In an expanding universe, galaxies that remain at constant values of x, y, and z in a proper reference frame will have constant separation. This is not the case, as Hubble's Law implies that the separation of galaxies at fixed (x, y, z) will increase proportionally to $a(t)$. Thus, to make a metric which is valid for a spatially flat universe, we replace $(dx^2 + dy^2 + dz^2)$ with $a^2(t)(dx^2 + dy^2 + dz^2)$. Converting to spherical coordinates (with χ as the radial distance, θ as the polar angle, and ϕ as the azimuthal angle) makes calculations easier, as cosmic measurements are made in terms of χ and these angles. Making the appropriate substitutions into equation (11) yields the following metric:

$$ds^2 = -(c\ dt)^2 + a^2(t)[d\chi^2 + \chi^2(d\theta^2 + \sin^2\theta\ d\phi^2)] \tag{12}$$

To account for a curved ($k \neq 0$) isotropic and homogeneous universe, χ must be replaced with $r(\chi)$, where [11]

$$r(\chi) \equiv \begin{cases} ck^{-1/2} \sin\left(\frac{k^{1/2}\chi}{c}\right), & k > 0; \\ c(-k)^{-1/2} \sinh\left[\frac{(-k)^{1/2}\chi}{c}\right], & k < 0; \\ \chi, & k = 0. \end{cases} \tag{13}$$

Replacing dt with $a(\tau)d\tau$ produces the final form of the Robertson-Walker metric that will be used:

$$ds^2 = a^2(\tau)[-c^2 d\tau^2 + d\chi^2 + r^2(\chi)(d\theta^2 + \sin^2\theta \; d\phi^2)] \tag{14}$$

Now consider the path of a photon emitted from $(\tau_{em}, \chi_{em}, \theta_{em}, \phi_{em})$ that follows a path of constant θ and ϕ (a radial path) to $(\tau_0, 0, \theta_{em}, \phi_{em})$. For light, $ds^2 = 0$ along any path. Also, for the light rays coming to the observer at $\chi = 0$ from distant sources, $d\theta = d\phi = 0$. Equation (14), for these conditions, reduces to

$$d\chi = \pm c \; d\tau \tag{15}$$

Because χ is decreasing and τ is increasing, the minus sign must be used. Integrating both sides of (15) over the path of the photon yields:

$$\chi_{em} = c(\tau_{obs} - \tau_{em}) \tag{16}$$

Equation (16), the light cone condition, provides a simple method for determining χ_{em} for an event given its $\Delta\tau$. This result that will be used later.

4 Cosmic Microwave Background Constraints

The cosmic microwave background (CMB) is blackbody radiation whose spectrum peaks in the microwave region. The anisotropy in CMB measurements is essentially a result of three phenomena. Two of them, namely the Doppler shift due to the Earth's motion and the foreground emission from the Milky Way, can be subtracted from the measurements to reveal the third source — residual fluctuations produced in the early universe.

Define τ_{rec} as the time after the big bang at which free electrons combined with protons to form the neutral hydrogen that fills the present universe. Because of the ionized gas that was present prior to τ_{rec}, photons were scattered. This scattering created an opaque surface on our backward light cone. (Everything we see when we look out across space is a part of our backward light cone.) Because of this surface, which we will refer to as the cosmic photosphere, events occurring at times before τ_{rec} cannot be observed.

If the cosmic photosphere were completely uniform, the CMB data (after subtraction) would be isotropic. However, the data still shows a lack of homogeneity arising from variations in temperature in the early universe. These variations result from fluctuations that occurred prior to τ_{rec} so no direct visual record of them can be obtained. However, the disturbances did give off sound waves, which traveled at a speed of approximately $c/2$ in the photon-baryon plasma without being scattered. These sound waves propagated to the intersection of the acoustic sphere and our backward light cone and left imprints (rings) in the CMB that can be measured. The acoustic sphere is the region around the source of a perturbation where sound waves from the perturbation can be found at a given time.

Consider two imprints made at time τ_{rec} on the cosmic photosphere (events A and B in Figure 2) caused by the same quantum perturbation (event E at time $\tau = 0$) and consider the spatial separation between them, L_{CMB}. Because the events are simultaneous, $\Delta\tau = 0$ between them. Because the cosmic photosphere is at a fixed χ, $\Delta\chi = 0$. Choosing an appropriate orientation for our reference frame, we can set $\Delta\phi = 0$. Finally, because $\chi_{rec} \gg$

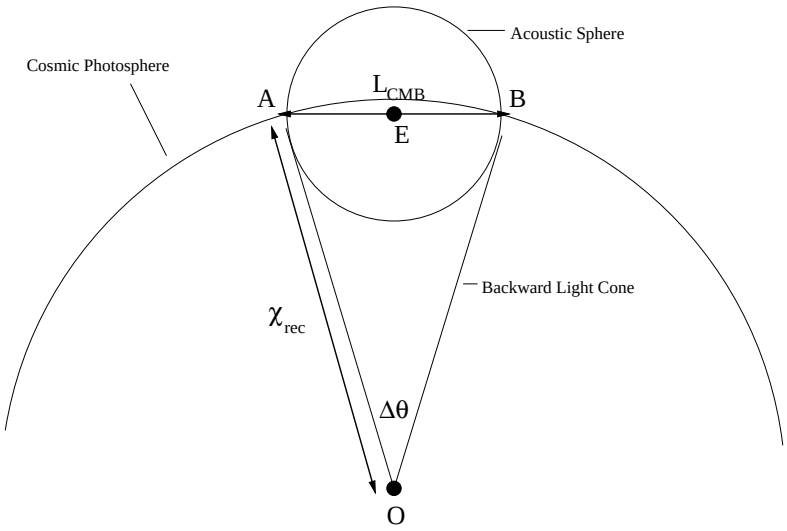

Figure 2: CMB measurements: (not to scale — in reality, $\chi_{rec} \gg L_{CMB}$) The acoustic sphere for an event E that occurs at $\tau = 0$ intersects with the backwards light cone on the cosmic photosphere at time τ_{rec} (events A and B). An observer with the shown light cone is at O. Event E actually occurs outside the cosmic photosphere, but this can't be seen in the diagram because of the lack of a time axis.

L_{CMB}, we know $\Delta\theta \ll 1$, and from equation (14) we have

$$L_{CMB} = \Delta s \approx a(\tau_{rec})\ r(\chi_{rec})\ \Delta\theta \tag{17}$$

The acoustic diameter L_{CMB} can also be measured in spherical coordinates with an origin at one of the events (assume it to be at event A). In this frame, $d\theta = d\phi = 0$ between A and B; $d\tau = 0$ as well because the events are still simultaneous. Sound travels at a speed of $\approx c/2$ in the photon-baryon plasma and both events were caused by a perturbation exactly half way between them at time $\tau = 0$, so their spatial separation is $D(A, B) = 2D(E, A) = 2\frac{c}{2}(\tau_A - \tau_E) = c\tau_{rec}$. Therefore,

$$L_{CMB} = \Delta s = a(\tau_{rec})\Delta\chi = c\ a(\tau_{rec})\ \tau_{rec} \tag{18}$$

Setting equation (17) equal to equation (18) yields

$$c\tau_{rec} = r(\chi_{rec})\Delta\theta \tag{19}$$

Hence,

$$\frac{c\tau_{rec}}{r(\chi_{rec})} = \Delta\theta \tag{20}$$

This $\Delta\theta$ is what cosmologists are effectively able to measure from the location of the first acoustic peak in the angular power spectrum [5].

To determine a theoretical value of $\Delta\theta$, we first introduce a dimensionless function $F \equiv H_0 r(\chi_{rec})/c$. Initially, we will consider only an open universe ($\Omega_m + \Omega_\Lambda < 1$). Equation (13) for $k < 0$ becomes:

$$F \equiv \frac{H_0 r(\chi_{rec})}{c} = H_0(-k)^{-1/2} \sinh\left[\left(\frac{-k}{H_0^2}\right)^{1/2} \frac{H_0\chi_{rec}}{c}\right] \tag{21}$$

Making the substitution $\Omega_k = -k/H_0^2$ into equation (21) yields:

$$F = \frac{1}{\sqrt{\Omega_k}} \sinh\left[\sqrt{\Omega_k}\frac{H_0\chi_{rec}}{c}\right] \tag{22}$$

From equations (16) and (10),

$$\frac{H_0\chi_{rec}}{c} = (H_0\tau_{obs} - H_0\tau_{rec}) = \int_{a_{rec}}^{1} \frac{dx}{\sqrt{\Omega_m x + \Omega_\Lambda x^4 + (\Omega_r h^2)h^{-2} - \Omega_k x^2}} \tag{23}$$

Substituting equation (23) for $H_0\chi_{rec}/c$ in equation (22) and using the fact that $a_{rec} = 1/1100$ [12] yields:

$$F = \frac{1}{\sqrt{\Omega_k}} \sinh\left[\sqrt{\Omega_k} \int_{1/1100}^{1} \frac{dx}{\sqrt{\Omega_m x + \Omega_\Lambda x^4 + (\Omega_r h^2)h^{-2} - \Omega_k x^2}}\right], \tag{24}$$

Similar derivations can be used for closed and flat universes to define F when $\Omega_m + \Omega_\Lambda \geq 1$.

From equation (10), we also know

$$H_0\tau_{rec} = H_0\tau(a_{rec}) = \int_0^{1/1100} \frac{dx}{\sqrt{\Omega_m x + \Omega_\Lambda x^4 + (\Omega_r h^2)h^{-2} - \Omega_k x^2}} \tag{25}$$

From equation (6) we know $\Omega_k = 1 - \Omega_m - \Omega_\Lambda - (\Omega_r h^2)h^{-2}$. We know $\Omega_\gamma h^2 = 2.4937 \times 10^{-5}$, where Ω_γ is the photon density parameter. The value of $\Omega_\gamma h^2$ value can be calculated from physical constants which are very precisely known and the accurately measured CMB temperature. To include neutrinos in the radiation density we use $\Omega_r = 1.68\Omega_\gamma$ [10], so the present value of the radiation parameter, which includes both photons and neutrinos, is constrained to $\Omega_r h^2 = 4.1894 \times 10^{-5}$. Substituting this into equations (24) and (25) and using $h = 0.7$m, currently the best approximation [13], leaves F and $H_0\tau_{rec}$ as functions of Ω_m and Ω_Λ only. Using equation (20) we can now define $\Delta\theta$, too, as a function of Ω_m and Ω_Λ.

$$\Delta\theta = G(\Omega_m, \Omega_\Lambda) \equiv \frac{c\tau(a_{rec})}{r(\chi_{rec})} = \frac{H_0\tau_{rec}}{F}, \tag{26}$$

where τ_{rec} is given by equation (25) and F is given by equation (24).

Figure 3 shows level curves of $G(\Omega_m,\ \Omega_\Lambda)$. Comparing the contours of Figure 3 with the orientation of the error region for CMB anisotropy data in figure (1) suggests that G accurately explains the orientation of the region, whose center is along the line $\Omega_m + \Omega_\Lambda = 1$. Furthermore, using the estimates $\Omega_m \approx \frac{1}{3}$ and $\Omega_\Lambda \approx \frac{2}{3}$, we can calculate $G(\frac{1}{3}, \frac{2}{3}) = \Delta\theta = .0206 = 1.18^\circ$. This agrees with the experimental value ($\Delta\theta \approx 1.2^\circ$).

5 Simplified Model for CMB Constraints

Consider equation (24). Plotting the integrand using approximate values for the omegas ($\Omega_m \approx \frac{1}{3}$ and $\Omega_\Lambda \approx \frac{2}{3}$) shows that its greatest contributions come from small values of x. Because the contribution of $\Omega_\Lambda x^4 + (\Omega_r h^2)h^{-2} - \Omega_k x^2$ in the radical is small relative to Ω_m for small values of x, these terms can be dropped to make an approximate calculation. The

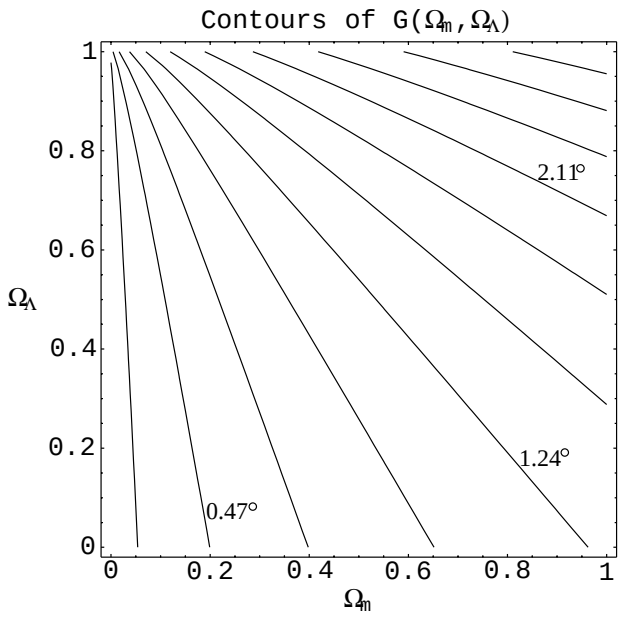

Figure 3: Level curves of $G(\Omega_m,\ \Omega_\Lambda) = \Delta\theta$: Note that the slope of the contours is negative throughout the region. Values of $\Delta\theta$ are provided in degrees. Also, in the region of $\Omega_m + \Omega_\Lambda = 1$, note that the slope $m \approx -1$.

contribution of $(\Omega_r h^2)h^{-2}$ to Ω_k is also relatively small (compared to contributions of Ω_m and Ω_Λ). Similarly, in equation (25) $\Omega_\Lambda x^4 - \Omega_k x^2$ can be ignored because it contributes much less to the radical than $\Omega_m + (\Omega_r h^2)h^{-2}$ (on the order of 10^{-3}). Eliminating these terms makes it possible to analytically evaluate the integrals and produce a more concise formula for $\Delta\theta$, albeit an approximation.

Using these simplifications for equations (24) and (25), define

$$\Delta\theta \approx G_s(\Omega_m, \Omega_\Lambda) \equiv \frac{2\sqrt{\Omega_k}(\sqrt{\Omega_m/1100 + \Omega_r} - \sqrt{\Omega_r})}{\Omega_m \sinh\left[\sqrt{\Omega_k}\left(\frac{2}{\sqrt{\Omega_m}} - 2\sqrt{\frac{1}{1100\Omega_m}}\right)\right]}, \quad \Omega_m + \Omega_\Lambda < 1 \tag{27}$$

This equation, like (24), is only valid for open universes, but similar equations can easily be derived for closed and flat universes. For $\Omega_\Lambda = \frac{2}{3}$ and $\Omega_m = \frac{1}{3}$, $G = 0.0216349$ and $G_s = 0.0204033$ — a 5.7% difference. Similar percent differences can be found on the rest of the Ω_m - Ω_Λ plane as long as Ω_m is not near 0. Though it is not clean, equation (27) provides a good approximation of $\Delta\theta$ using only elementary functions and arithmetic.

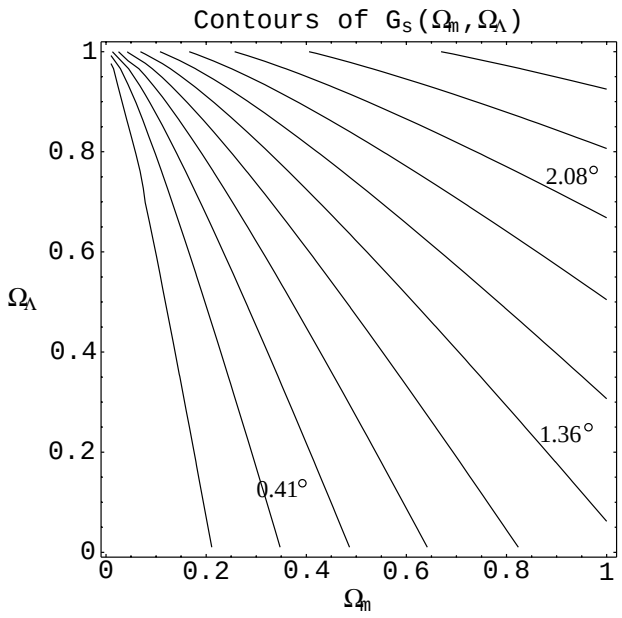

Figure 4: Level curves of $G_s(\Omega_m, \Omega_\Lambda)$ Note that the approximation matches less with Figure (3) at low values of Ω_m.

6 Constraints from Type Ia Supernovae

Now we turn our attention to the constraints obtained from measurements of Type Ia supernovae (SNe Ia). SNe Ia are the most luminous and homogeneous of all supernova types, and are therefore excellent standard candles that can be used for measurements. The calculations here will be similar to those made in the CMB section, but now we will be looking at ratios of different F's instead of ratios of τ to F.

Because all SNe Ia are believed to have almost the same peak power, when corrected for the shape of the light curve [2], we can consider two supernovae with the same emitted power ($P_1 = P_2$) at $a_{em} = a_1$ and $a_{em} = a_2$. The measured luminosity flux of each supernova is related to the power, time, and distance of emission as follows:

$$\Phi = \frac{P_{em} a_{em}^2}{4\pi r^2(\chi_{em})}, \tag{28}$$

The ratio of the fluxes of the two supernovae is therefore

$$\frac{\Phi_2}{\Phi_1} = \frac{P_2}{P_1}\left(\frac{a_2}{a_1}\right)^2 \frac{r^2(\chi_1)}{r^2(\chi_2)} \approx \left(\frac{a_2}{a_1}\right)^2 \frac{r^2(\chi_1)}{r^2(\chi_2)}. \tag{29}$$

Though Φ_1 and Φ_2 themselves are not precisely known, the ratio between them, Φ_2/Φ_1 can be measured. All the uncertainty in supernova calculations arises from the assumption $P_1 = P_2$, which is only accurate to within 10-20% [2].

Consider equations (22) and (23) with χ_{rec}, a_{rec}, and τ_{rec} replaced with $\chi_{1,2}$, $a_{1,2}$, and $\tau_{1,2}$. With these substitutions, the flux ratio becomes

$$\frac{\Phi_2}{\Phi_1} = \left[\frac{F(\Omega_m, \Omega_\Lambda, a_1)}{F(\Omega_m, \Omega_\Lambda, a_2)}\right]^2 \left(\frac{a_2}{a_1}\right)^2. \tag{30}$$

Now define

$$f(\Omega_m, \Omega_\Lambda) \equiv \ln\left(\frac{\Phi_2}{\Phi_1}\right), \tag{31}$$

for a given a_1 and a_2. Figures (5) through (9) show level curves of f for different values of a_1 and a_2. The contours in these figures are spaced so that an interval of plus or minus one contour corresponds to the error from a 10% uncertainty in flux calibration (denser contours correspond to less uncertainty).

From the figures, we see that greater values of Δa, such as those found in Figures 5, 8, and 9 correspond to less uncertainty. Analyzing the contributions to $f(\Omega_m, \Omega_\Lambda)$ can also show this. Figures 6 and 7 closely model and explain the orientation of the error ellipse for SNe Ia in Figure 1. This is due to the fact that the experimental data from [1] and [2] dealt with supernovae at redshifts $0.16 \leq z \leq 0.86$, which, using the fact that $z = (1/a) - 1$, corresponds to $0.54 \leq a \leq 0.86$.

Note that no simplified model can easily be constructed because the relatively large values of a_{em} used here result in all the terms in integrals having relatively equal importance over the region of integration.

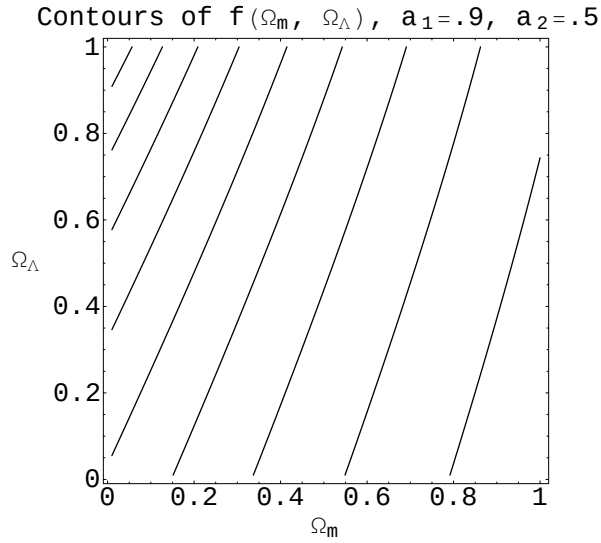

Figure 5: Level curves of $f(\Omega_m, \Omega_\Lambda)$ for $a_1 = .9$ and $a_2 = .5$ (One near and one distant supernova).

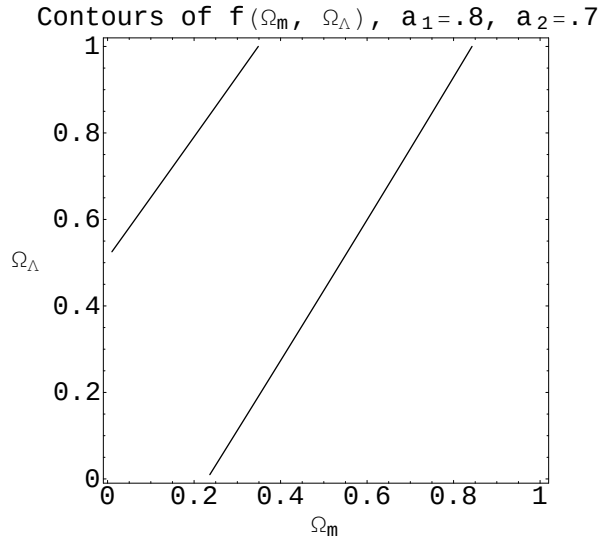

Figure 6: Level curves of $f(\Omega_m, \Omega_\Lambda)$ for $a_1 = .8$ and $a_2 = .7$ (Two supernovae with relatively small $\Delta\tau$ between them).

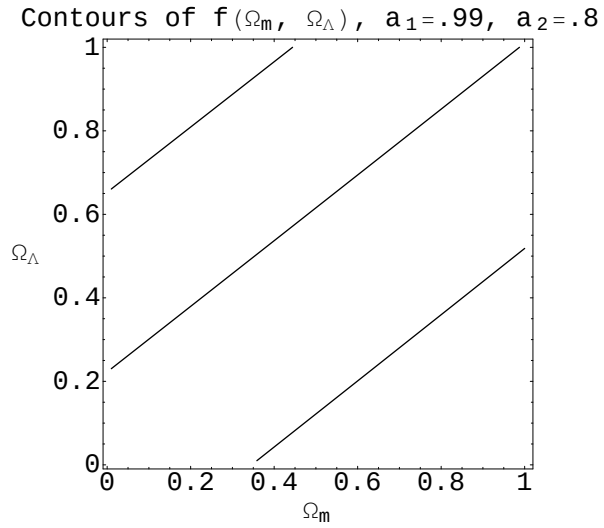

Figure 7: Level curves of $f(\Omega_m, \Omega_\Lambda)$ for $a_1 = .99$ and $a_2 = .8$ ($a_1 = .99$ corresponds to a supernova closer than any used in [1] and [2].)

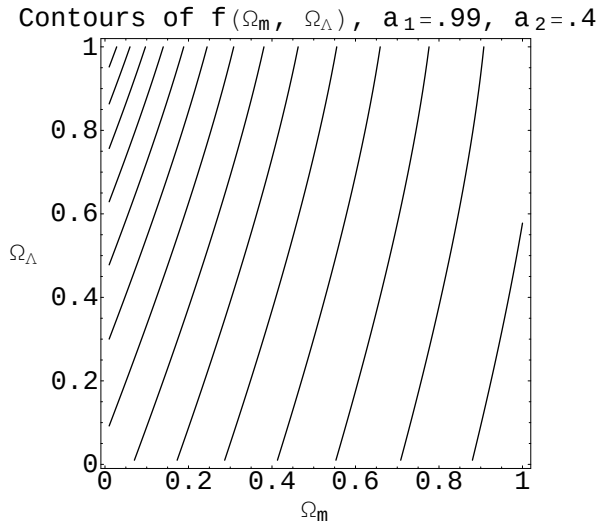

Figure 8: Level curves of $f(\Omega_m, \Omega_\Lambda)$ for $a_1 = .99$ and $a_2 = .4$. The supernova at $a = .4$ ($z \approx 1.7$) corresponds to the furthest measured supernova to date. [14]

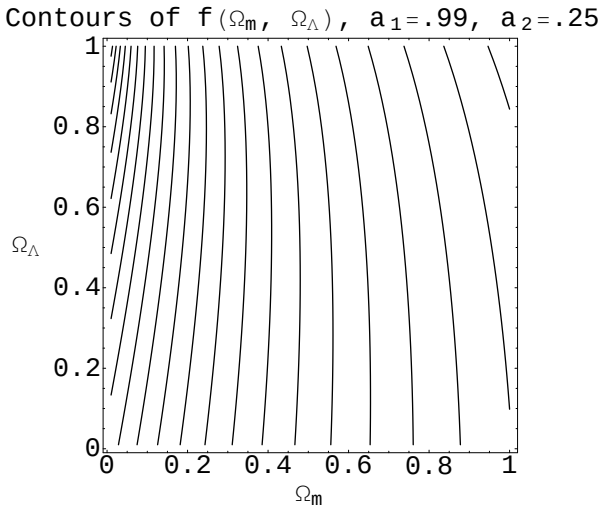

Figure 9: Level curves of $f(\Omega_m, \Omega_\Lambda)$ for $a_1 = .99$ and $a_2 = .25$. Finding a supernova at $a = .25$ would help increase the constraints on Ω_m and Ω_Λ) by a significant amount.

7 Conclusion

The level curves of the functions G and f accurately explain the plotted error curves obtained from data. This suggests that the derived equations, namely equations (26) and (30), accurately describe the physical phenomena of cosmic microwave background and supernova luminosity flux and are capable of reproducing the results of the SNe Ia and CMB projects (Figure 1). These equations can now be used to predict how possible future observations will affect constraints on Ω_m and Ω_Λ. Discovery of a high-redshift supernova (large z, small a) would create constraints with error ellipses having major axes in the direction of the contours in in Figures 8 and 9, which are nearly vertical and have much less error compared to the contours in Figures 5, 6, and 7. This could feasibly allow Ω_m and Ω_Λ to be constrained to a small area with SNe Ia data alone, because this new narrow vertical ellipse would intersect the oblique ellipse for SNe Ia in Figure 1. Also, if improvements are made on the measured value of $\Delta\theta$ for cosmic microwave background data, equation (26) would predict the effect

of the change on Ω_m and Ω_Λ.

8 Acknowledgments

I would like to thank the Center for Excellence in Education (CEE) for providing me with the opportunity to carry out my research. I also thank Eric Sheu for his assistance in writing this paper and Ben Rahn for his assistance in editing. Finally, I extend my deepest thanks to Dr. Edmund Bertschinger, whose support and guidance made this project possible.

References

[1] S. Perlmutter et al, Astrophyw. J., **517**, 565 (1999).

[2] A.G. Riess et al., Astron. J., **116**, 1009 (1998); and astro-ph/0104455.

[3] M.S. Turner, Cosmology Update (1998) (astro-ph/9901168).

[4] S.N. Caroll, W.H. Press, and E.L. Turner, Ann. Rev. Astron. Astrophys. **30**, 499 (1992)

[5] S. Hanany et al., Astrophys. J., **545**, L5 (2000); and astro-ph/0104459

[6] P. de Bernardis et al., Nature, **404**, 955 (2000); and astro-ph/0105296

[7] N.W. Halverson et al., astro-ph/0104489; and C. Pryke et al., astro-ph/0104490

[8] The High-Z SN Search. <http://cfa-www.harvard.edu/cfa/oir/Research/supernova/public.html>

[9] A.G. Riess, Publ. Astron. Soc. Pacific, **112**, 1284 (2000)

[10] J. Bernstein, An Introduction to Cosmology. Prentice Hall, Englewood Cliffs (1995).

[11] E. Bertschinger, Cosmography in a Robertson-Walker Universe (1999).

[12] J.A. Peacock, Comological Physics. Cambridge University Press (1999).

[13] W.L. Freedman et. al., Astrophys. J., **525**, 80 (1999)

[14] A.G. Riess et. al. (2001) (astro-ph/0104455)